

QUANTUM DOTS

PACS numbers: 73.21.La; 78.67.Hc; 42.65.–k
DOI: 10.1070/QE2013v043n01ABEH014731

Optical absorptions of the low-lying states with higher angular momenta of a D^- system in a spherical quantum dot

Wenfang Xie

Abstract. **Optical absorptions of the low-lying states with higher angular momenta of the D^- system in a spherical quantum dot (QD) with the Gaussian potential are studied by using the matrix diagonalisation method and the compact density-matrix approach. The linear, nonlinear third-order and total optical absorption coefficients are calculated for the $^1P^- \rightarrow {}^1D^+$ and $^1D^+ \rightarrow {}^1F^-$ transitions. Numerical results for GaAs/$Ga_{1-x}Al_xAs$ QDs are presented. The calculated results show that with increasing quantum numbers describing the angular momenta of transitions the optical absorption peaks shift towards lower energies and their intensities increase.**

Keywords: *quantum dot, negative-donor system, excited states.*

1. Introduction

A negative-donor system (D^-) is similar to the H^- ion, which is an interesting example of a few-particle system where the electron–electron interaction plays a decisive role in confining and trapping a second electron [1]. The D^- system is one of the simplest many-electron systems which cannot be described exactly. Because the three-dimensional D^- binding energy is very weak, its observation is possible only at very low temperatures. This situation limits to some extent the application of such systems in semiconductor. Recently, semiconductor quantum dots (QDs) have aroused considerable interest, and electron–electron interactions have been shown to be of great importance in such systems. Since the QDs have atomic-like discrete energy levels and their optical properties can be controlled by modifying the dot size, the QD systems are expected to be applied as novel optical devices. Such microstructures confine charged particles in all three space dimensions. The reduced dimensionality enhances considerably the binding energy of D^-, and thus facilitates the experimental observations.

On the other hand, impurities in semiconductors influence both transport and optical properties and therefore confined D^- systems in low-dimensional semiconductors have attracted considerable interest. The existence of D^- centres in centre-doped GaAs/AlxGa$_{1-x}$As multiple quantum wells was first reported by Huant et al. [1] in 1990. Since then many experimental [2–4] and theoretical [5–16] investigations for D^- centres in quantum wells and QDs have been carried out. Most of these works are related to the electronic states and the binding energies of the D^- systems in the low-dimensional semiconductors. Recently, Sahin [17] investigated the nonlinear optical properties of the D^- center in a spherical QD. He found that the size of the QD has drastic effects on nonlinear optical properties.

The nonlinear optical properties are of particular interest, since they provide detailed information about the microscopic interactions of the confined systems. In semiconductor QDs, the nonlinear optical properties associated with optical absorptions are known to be greatly enhanced as compared to nonlinearity in bulk semiconductors. Hence, the nonlinear optical properties of QDs have been investigated both experimentally and theoretically by many authors [18–22]. To the best of our knowledge, most works on the optical absorptions of QDs have concentrated on the calculation of the transitions between the ground and the first excited states [17, 23]. A study of the optical absorptions of the low-lying states with higher angular momenta in QDs is still lacking. Therefore, studies in this field are still important for both theoretical research and practical applications.

From the point of view of the nonlinear optical properties of QDs, the analysis of D^- systems is inevitable because the confinement of electrons in such structure leads to the enhancement of the electron–electron and electron–impurity interactions. Hence, in the present study, we will focus on studying the optical absorptions of the low-lying states with higher angular momenta of the D^- system for the spin-singlet states in QDs. By using the matrix diagonalisation method and the compact density-matrix approach, we will calculate the linear, nonlinear third-order and total absorption coefficients (ACs) and refractive index (RI) changes for the $^1P^- \rightarrow {}^1D^+$ and $^1D^+ \rightarrow {}^1F^-$ transitions in QDs. Furthermore, we will investigate the effects of the well depth and the range of the confinement potential for the optical absorptions of the low-lying states with higher angular momenta of the D^- system in a spherical QD.

2. Theory and formulation

In considering two electrons bound to an ionised donor localised in a QD, the Hamiltonian of the system can be given by

$$H = \sum_{i=1,2}\left[\frac{\boldsymbol{p}_i^2}{2m_e} + V_{conf}(r_i) - \frac{e^2}{\varepsilon r_i}\right] + \frac{e^2}{\varepsilon r_{12}}, \qquad (1)$$

where m_e is the effective mass of an electron; $\boldsymbol{p}_i$ and $\boldsymbol{r}_i$ denote the momentum and the radius vector of the ith electron, respectively; $r_{12} = |\boldsymbol{r}_1 - \boldsymbol{r}_2|$ is the electron–electron separation; $V_{conf}(r_i)$ is the confinement potential; and $\varepsilon = 4\pi\varepsilon_0\varepsilon_r$ is the

Wenfang Xie School of Physics and Electronic Engineering, Guangzhou University Guangzhou 510006, P.R. China; e-mail: xiewf@vip.163.com

Received 27 September 2011; revision received 27 June 2012
Kvantovaya Elektronika **43** (1) 71–75 (2013)
Submitted in English

dielectric constant of the medium in which the electrons are moving.

To calculate the confinement strength and its dependence on the distance from QDs, we assume that the confining potential has the Gaussian form [24], i.e.,

$$V_{\text{conf}}(r) = -V_0 \exp[-(r/R)^2], \tag{2}$$

where V_0 is the depth of the confinement potential ($V_0 > 0$) and R is the radius of the QD. Due to the smoothly varying form, finite depth and radius given by equation (2), the Gaussian potential is a good approximation of the confinement potential in electrostatic QDs [25], in which the confinement results from an inhomogeneous electric field. In self-assembled QDs with a composition modulation [26], the confinement potential can be approximated by the Gaussian potential [27].

Let $^{2S+1}L^{\pi}$ denote the quantum state because the total angular momentum L, the parity π (in the following e and o represent the even parity and odd parity, respectively), and the total spin S of two electrons are the good quantum numbers. As is known, the two electrons obey Fermi–Dirac statistics which means that the electronic part of the total wave function must be antisymmetric, i.e., when $S = 0$, the spatial part of the electronic wave function must be symmetric, and when $S = 1$, the spatial part of the electronic wave function must be antisymmetric.

To obtain the eigenfunctions and the eigenenergies associated with the D^- centre in a spherical QD, we diagonalised the Hamiltonian of the D^- centre in a model space spanned by translational invariant harmonic product states

$$\Phi_{[K]}^{LS\pi} = \sum_{[K]} \tilde{A}\{[\varphi_{n_1 l_1}^{\omega}(\boldsymbol{r}_1)\varphi_{n_2 l_2}^{\omega}(\boldsymbol{r}_2)]_{L\pi}\chi_S\}, \tag{3}$$

where

$$\chi_S = [\zeta(1)\zeta(2)]_S; \tag{4}$$

$\zeta(i)$ is the spin state of the ith electron and the spins of two electrons are coupled to S; φ_{nl}^{ω} is a three-dimensional harmonic oscillator state with a frequency ω and an energy $(2n + l + 3/2)\hbar\omega$; $\tilde{A}$ is the antisymmetriser; and $[K]$ denotes the whole set of quantum numbers (n_1, l_1, n_2, l_2) with $l_1 + l_2 = L$ being the total angular momentum. The angular momentum L is odd if the spin $S = 1$ and is even if the spin $S = 0$ such that the wave function is antisymmetric. The exact diagonalisation method consists in spanning the Hamiltonian for a given basis and extracting the lowest eigenvalues of the matrix generated. The calculation of matrix elements is realised by using three-dimensional coefficients [28].

Since the whole set of eigenstates of the harmonic product basis forms a complete basis in the Hilbert space, the procedure of increasing the number of linearly independent eigenstates converges to the exact result. The limits are set only by the capacity of the computer to diagonalise $N \times N$ Hermitean matrices. On the other hand, we are interested only in the low-lying states and in the qualitative aspects, the model space adopted being neither very large to facilitate numerical calculations nor very small to ensure qualitative accuracy. This is achieved by extending the dimension of the model space step by step; in each step the new results are compared with previous results from a smaller space, until satisfactory convergence is achieved. After the diagonalisation we obtain the eigenvalues and eigenstates. Evidently, the eigenvalues and the eigenfunctions depend on the adjustable parameter Ω. In practice, Ω serves as a variational parameter to minimise the eigenvalues.

The optical absorption calculation is based on Fermi's golden rule, for which the total optical AC is given by [17]

$$\alpha(\nu, I) = \alpha^{(1)}(\nu) + \alpha^{(3)}(\nu, I), \tag{5}$$

where

$$\alpha^{(1)}(\nu) = 2\pi\nu\sqrt{\frac{\mu}{\varepsilon_{\text{r}}}}\frac{\sigma_{\text{s}} e^2 |M_{\text{fi}}|^2 \hbar\Gamma_{\text{fi}}}{(h\nu - \Delta E_{\text{fi}})^2 + (\hbar\Gamma_{\text{fi}})^2} \tag{6}$$

and

$$\alpha^{(3)}(\nu, I) = -4\pi\nu\sqrt{\frac{\mu}{\varepsilon_{\text{r}}}}\frac{\sigma_{\text{s}} I e^4 |M_{\text{fi}}|^4 \hbar\Gamma_{\text{fi}}}{n_{\text{r}}\varepsilon_0 c[(h\nu - \Delta E_{\text{fi}})^2 + (\hbar\Gamma_{\text{fi}})^2]^2} \tag{7}$$

are the linear and nonlinear third-order optical ACs, respectively; $\Delta E_{\text{fi}} = E_{\text{f}} - E_{\text{i}}$ is the energy difference between the lower and upper levels; c is the speed of light; I is the incident optical intensity; σ_{s} is the electron density; μ is the permeability of the system; n_{r} is the refractive index of the semiconductor; $\varepsilon_{\text{r}} = n_{\text{r}}^2\varepsilon_0$ is the real part of the permittivity; and $M_{\text{fi}} = \langle \text{f}|\boldsymbol{r}_1 + \boldsymbol{r}_2|\text{i}\rangle$ is the electric dipole moment of the transition from the i state to the f state in a QD. The nondiagonal matrix element Γ_{fi} ($\text{f} \neq \text{i}$) of the phenomenological operator Γ, which is called the relaxation rate of the f and i states, is the inverse of the relaxation time T_{fi} for these states, namely $\Gamma_{\text{fi}} = 1/T_{\text{fi}}$.

From the expression of the spherical harmonic

$$Y_{lm}(\theta,\varphi)\cos\theta = B_{l-1\,m}Y_{l-1\,m}(\theta,\varphi) + B_{lm}\text{Y}_{l+1\,m}(\theta,\varphi), \tag{8}$$

where

$$B_{lm} = \left[\frac{(l+1)^2 - m^2}{(2l+1)(2l+3)}\right]^{1/2}, \tag{9}$$

we can obtain

$$\langle n'l'm'|r\cos\theta|nlm\rangle = (B_{l-1\,m}\delta_{l'l-1} + B_{lm}\delta_{l'l+1})U_{nln'l'}\delta_{m'm}, \tag{10}$$

where

$$U_{nln'l'} = \int_0^{\infty} R_{nl}(r)R_{n'l'}(r)r^3\text{d}r. \tag{11}$$

The dipole transition must occur between the states of different parity. On the other hand, the dipole operator is independent of the electron spin. The dipole-allowed optical transitions always result from the same spin states. Hence, we restrict our study to the $^1S^+ \rightarrow {}^1P^-$, $^1P^- \rightarrow {}^1D^+$ and $^1D^+ \rightarrow {}^1F^-$ transitions of the spin-singlet states.

3. Numerical results

All the calculations were performed using the following parameters: $m_{\text{e}} = 0.067m_0$ (m_0 is the free electron mass), $\varepsilon = 13.18$, $\sigma_{\text{s}} = 5.0\times10^{24}$ m^{-3}, $\Gamma_{\text{fi}} = (1/0.14)$ ps^{-1}, and $n_{\text{r}} = 3.2$.

These parameters correspond to GaAs/$Ga_{1-x}Al_xAs$ QDs. To derive the well depths, we assume that the band gap discontinuity in a GaAs/$Ga_{1-x}Al_xAs$ QD is distributed about 60% on the conduction band and 40% on the valence band, with the total band-gap difference ΔE_g (in eV) given as a function of Al concentration x as $\Delta E_g = 1.247x$ [29].

Figure 1 shows the linear ACs of the D^- system confined in a spherical QD with the well depth $V_0 = 112.23$ meV as a function of the incident photon energy for the $^1S^+ \rightarrow {}^1P^-$, $^1P^- \rightarrow {}^1D^+$ and $^1D^+ \rightarrow {}^1F^-$ transitions, respectively, for the dot radius $R = 10$ nm. We note that, as the angular momentum quantum number L of the transition states increases, the linear AC peak positions shift to lower energies (red shift). This red shift occurs because the energy difference ΔE_{fi} between the lower and upper states will decrease with increasing L. One can see from Fig. 1 that the peak values of the linear ACs of the $^1P^- \rightarrow {}^1D^+$ and $^1D^+ \rightarrow {}^1F^-$ transitions are one–two orders of magnitude higher than that in the case of the $^1S^+ \rightarrow {}^1P^-$ transition. One physical origin of this result is that the overlapping of the wave functions between the lower and upper states increases with increasing L. The dipolar transition matrix element will increase with increasing L, thereby leading to an increase in the linear optical ACs. Another reason is that the transition probability will increase because the energy difference between the lower and upper states decreases with increasing L, thereby leading to a considerable increase in the optical. If it is desired to obtain a larger optical absorption, then an excited state transition should be employed.

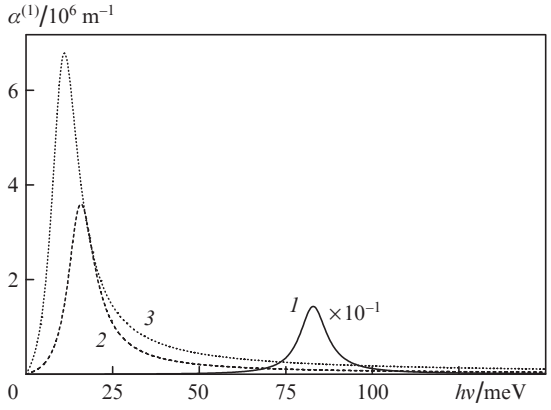

Figure 1. Linear ACs of the D^- spin-singlet states confined in a spherical GaAs/$Ga_{1-x}Al_xAs$ QD as a function of the incident photon energy for the (*1*) $^1S^+ \rightarrow {}^1P^-$, (*2*) $^1P^- \rightarrow {}^1D^+$, and (*3*) $^1D^+ \rightarrow {}^1F^-$ transitions at $V_0 = 112.23$ meV and $R = 10$ nm.

In order to investigate the confinement effect of the well depth on the optical absorptions of the excited states, we plotted (Fig. 2) the linear, nonlinear third-order and total optical ACs of the $^1P^- \rightarrow {}^1D^+$ transition as a function of the incident photon energy for a spherical QD with different well depths, corresponding to different Al concentrations [29] at $R = 10$ nm and $I = 1.5\times10^9$ W m^{-2}. It is found that the confinement effect of the well depth (i.e., Al concentration) for the ACs is significant. It can be seen that the linear, nonlinear third-order and total AC peak positions shift to higher energies (blue shift) with increasing V_0. This blue shift occurs because the energy difference between the lower and upper states will increase with increasing V_0. Figure 2 also shows that the absorption peak intensity increases with increasing V_0, i.e., the larger the well depth of the confinement potential, the sharper the absorption peak and the bigger the absorption peak intensity. The physical origin is that the transition matrix element increases with increasing V_0. Although for the $^1D^+ \rightarrow {}^1F^-$ transition the large change in the total AC is due to the linear term, the nonlinear third-order term, which is out-of-phase with the linear term, has also a large contribution in the total AC with increasing V_0.

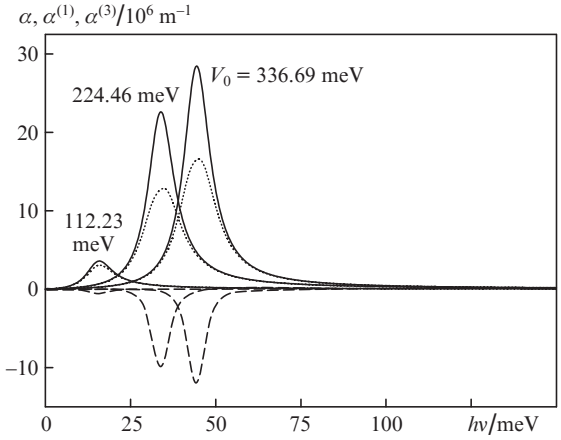

Figure 2. Linear [$\alpha^{(1)}$, solid curves], nonlinear third-order [$\alpha^{(3)}$, dashed curves] and total (α, dotted curve) optical ACs for the $^1P^- \rightarrow {}^1D^+$ transition as a function of the incident photon energy for different V_0 (GaAs/$Ga_{1-x}Al_xAs$ QDs, $R = 10$ nm, and $I = 1.5\times10^9$ W m^{-2}).

The influence of the dot size on the optical absorptions of the excited states is presented in Fig. 3. The figure shows the linear, nonlinear third-order and total optical ACs of the $^1P^- \rightarrow {}^1D^+$ transition as a function of the incident photon energy for a spherical QD with different dot radii R at the well depth $V_0 = 112.23$ meV and the incident optical intensity $I = 1.5\times10^9$ W m^{-2}. The figure explains the quantum size effect for the optical absorption of the excited state. One can see

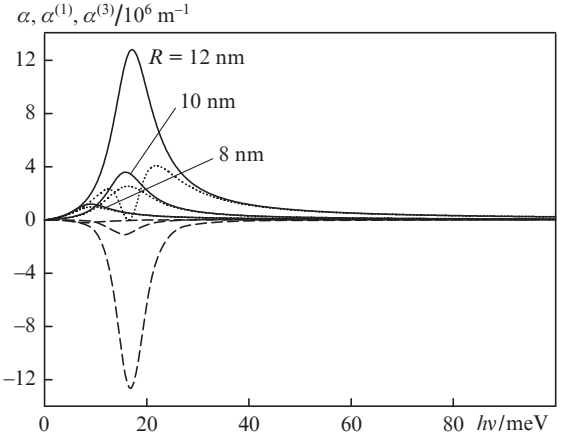

Figure 3. Linear [$\alpha^{(1)}$, solid curves], nonlinear third-order [#(3), dashed curves] and total (α, dotted curve) optical ACs for the $^1P^- \rightarrow {}^1D^+$ transition as a function of the incident photon energy for different R (GaAs/$Ga_{1-x}Al_xAs$ QDs, $V_0 = 112.23$ meV, and $I = 1.5\times10^9$ W m^{-2}).

that the increase in the radius of QDs leads to the increase in the maximum values of corresponding ACs. As the radius of QDs increases, the all ACs peak positions will move to the right side, which indicates a dot-radius-induced blue shift of the resonance in QDs. Therefore, the radius of QDs has an important influence on the optical absorptions of the excited states.

In order to see the optical absorptions of the higher excited-state transitions, Fig. 4 demonstrates the linear, nonlinear third-order and total optical ACs of the $^1D^+ \rightarrow {}^1F^-$ transition as a function of the incident photon energy for different values of V_0 and $I = 3.0\times10^9$ W m^{-2}. The variations of all the ACs are qualitatively similar to those observed in Fig. 2. However, one can see from Fig. 4 that the optical absorptions are stronger in the $^1D^+ \rightarrow {}^1F^-$ transition than in the $^1P^- \rightarrow {}^1D^+$ transition and consequently, for the same value of V_0, the AC is larger in the $^1D^+ \rightarrow {}^1F^-$ transition than in its $^1P^- \rightarrow {}^1D^+$ counterpart. Comparison of the curves in Figs 2 and 4 shows that the linear AC and the absolute value of the nonlinear third-order AC as well as the total AC increase with increasing angular momentum quantum number L of the transition.

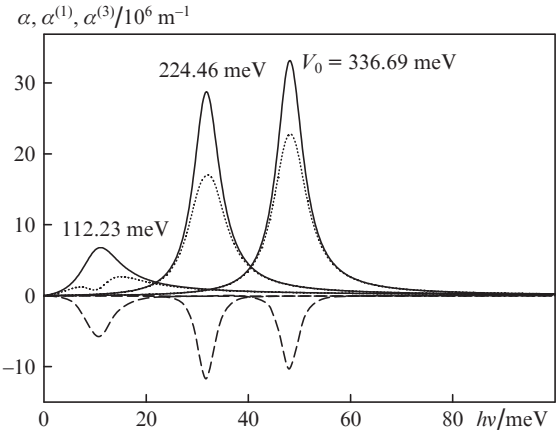

Figure 4. Linear [$\alpha^{(1)}$, solid curves], nonlinear third-order [$\alpha^{(3)}$, dashed curves] and total (α, dotted curve) optical ACs for the $^1D^+ \rightarrow {}^1F^-$ transition as a function of the incident photon energy for different V_0 (GaAs/$Ga_{1-x}Al_xAs$ QDs, R = 10 nm, and $I = 3.0\times10^9$ W m^{-2}).

Figure 5 shows the linear, nonlinear third-order and total optical ACs of the $^1D^+ \rightarrow {}^1F^-$ transition as a function of the incident photon energy for different dot radii R and $I = 3.0\times10^9$ W m^{-2}. The variations of the ACs are qualitatively similar to those observed in Fig. 3.

Thus, we have calculated the linear, nonlinear third-order and total optical ACs for $^1P^- \rightarrow {}^1D^+$ and $^1D^+ \rightarrow {}^1F^-$ transitions as a function of the incident photon energy. The results show that with increasing angular momentum quantum numbers of transitions, the optical AC peaks shift towards lower energies and the absorption intensities increase. Hence, in order to obtain the larger optical absorptions, we can employ the higher excited state transitions. To our knowledge, there are only few studies on the absorption spectra including the transitions between higher electronic states of a D^- system in QDs. Because such studies are missing, we believe that our study makes an important contribution to the solution of this problem.

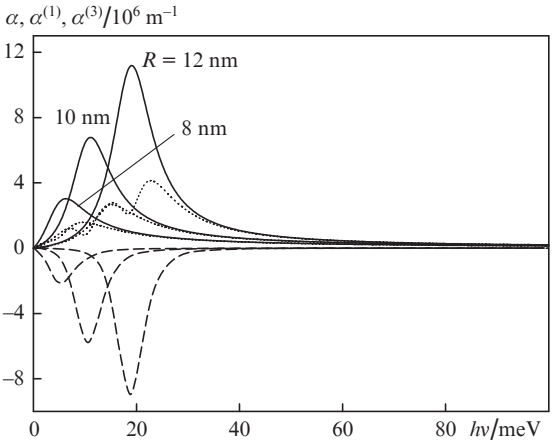

Figure 5. Linear [$\alpha^{(1)}$, solid curves], nonlinear third-order [$\alpha^{(3)}$, dashed curves] and total (α, dotted curve) optical ACs for the $^1D^+ \rightarrow {}^1F^-$ transition as a function of the incident photon energy for different R (GaAs/$Ga_{1-x}Al_xAs$ QDs, V_0 = 112.23 meV, and $I = 3.0\times10^9$ W m^{-2}).

Acknowledgements. This work is financially supported by the National Natural Science Foundation of China (Grant No. 11074055).

References

1. Huant S., Najda S.P., Etienne B. *Phys. Rev. Lett.*, **65**, 1486 (1990).
2. Holmes S., Cheng J.P., McCombe B.D., Schaff W. *Phys. Rev. Lett.*, **69**, 2571 (1992).
3. Lok J.G.S., Geim A.K., Maan J.C., Marmorkos I., Peeters F.M., Mori N., Eaves L., Foster T.J., Main P.C., Sakai J.W., Henini M. *Phys. Rev. B*, **53**, 9554 (1996).
4. Jiang Z.X., McCombe B.D., Zhu J.L., Schaff W. *Phys. Rev. B*, **56**, R1692 (1997).
5. Larsen D.M., McCann S.Y. *Phys. Rev. B*, **46**, 3966 (1992).
6. Dzyubenko A.B., Sivachenko A.Y. *Phys. Rev. B*, **48**, 14690 (1993).
7. Shi J.M., Peeters F.M., Devreese J.T. *Phys. Rev. B*, **51**, 7714 (1995).
8. Chen R., Bajaj K.K., Cheng J.P., McCombe B.D. *Phys. Rev. B*, **51**, 9825 (1995).
9. Herbert L.F., David M.L. *Phys. Rev. B*, **52**, 16937 (1995).
10. Kanamaru S., Tokuda N. *Phys. Rev. B*, **55**, 4516 (1997).
11. Marmorkos I.K., Schweigert V.A., Peeters F.M. *Phys. Rev. B*, **55**, 5065 (1997).
12. Szafran B., Adamowski J., Stebe B. *J. Phys. Condens. Matter*, **10**, 7575 (1998).
13. Riva C., Schweigert V.A., Peeters F.M. *Phys. Rev. B*, **57**, 15392 (1998).
14. Xie W.F. *J. Phys. Condens. Matter*, **12**, 3849 (2000).
15. Ruan W.Y., Chan K.S., Pun E.Y.B. *Phys. Rev. B*, **63**, 205204 (2001).
16. Daries Bella R.S., Navaneethakrishnan K. *Solid State Commun.*, **130**, 773 (2004).
17. Sahin M. *J. Appl. Phys.*, **106**, 063710 (2009).
18. Baskoutas S., Paspalakis E., Terzis A.F. *Phys. Rev. B*, **74**, 153306 (2006).
19. Baskoutas S., Paspalakis E., Terzis A.F. *J. Phys. Condens. Matter*, **19**, 395024 (2007).
20. Yilmaz S., Safak H. *Physica E*, **36**, 40 (2007).
21. Karabulut I., Atav J., Safak H., Tomak M. *Eur. Phys. J. B*, **55**, 283 (2007).
22. Karabulut I., Baskoutas S. *J. Appl. Phys.*, **103**, 073512 (2008).
23. Xie W.F. *Opt. Commun.*, **284**, 1872 (2011).
24. Adamowski J., Kwasniowski A., Szafran B. *J. Phys. Condens. Matter*, **17**, 4489 (2005).

25. Bednarek S., Szafran B., Lis K., Adamowski J. *Phys. Rev. B*, **68**, 155333 (2003).
26. Siverns P.D., Malik S., McPherson G., Childs D., Roberts C., Murray R., Joyce B.A., Davock H. *Phys. Rev. B*, **58**, R10127 (1998).
27. Szafran B., Bednarek S., Adamowski J. *Phys. Rev. B*, **64**, 125301 (2001).
28. Tobocman W. *Nuclear Physics A*, **357**, 293 (1981).
29. Bose C., Sarkar C.K. *Phys. Status Solidi B*, **218**, 461 (2000).